Future Foods 6 (2022) 100193

Contents lists available at ScienceDirect

Future Foods

journal homepage: www.elsevier.com/locate/fufo

Maillard reaction between pea protein isolate and maltodextrin via wet-heating route for emulsion stabilisation

Zijia Zhang [a,*], Bo Wang [b], Benu Adhikari [a,*]

[a] School of Science, RMIT University, Melbourne, VIC 3083, Australia
[b] School of Behavioural and Health Science, Australian Catholic University, Sydney, NSW 2060, Australia

ARTICLE INFO

Keywords:
Pea protein isolate
Maltodextrin
Maillard reaction
Conjugation
Solubility
Emulsion

ABSTRACT

Pea protein isolate (PPI)-maltodextrin (MD) conjugates were prepared by using controlled Maillard reaction at 90 °C in the solution state (wet-heating route). The degree of conjugation between PPI and MD was measured in terms of evolved colour, UV absorbance, and molecular weight change. Results showed that the degree of Maillard reaction increased with the increase in pH and reaction time; however, the PPI-MD conjugation was optimised and was successfully controlled within the initial stage at pH 7.5 and 8.0 to avoid the formation of melanonids. The random coil content of PPI significantly increased upon conjugation with MD producing more flexible structure. The functional properties of PPI in terms of solubility, surface change (zeta-potential), and emulsifying properties of PPI were significantly improved after conjugation with MD. The highest solubility PPI-MD conjugates was observed at 5 h of reaction. The canola oil-in-water (O/W) emulsion stabilised by PPI-MD 5 h conjugate at 2% of emulsifier concentration and homogenised at 60 MPa for 3 passes had the highest physical stability when subjected to 25–60 °C. These findings indicate that Maillard reaction can be controlled in the initial stage via the wet-heating route and the resulting conjugates can be much effective emulsifiers than plant proteins.

1. Introduction

Human population is predicted to grow to 9.7 billion by 2050 (United Nations, 2019). This rapidly rising population will ultimately put increasing pressure on the quantity as well as the quality of human diet. Consequently, the concern on the sustainability of animal-based food products has been driving the development and consumption of either entirely (vegan) or a high proportion of plant-based food products. For instance, about 2.5 million Australians (12.1%) are consuming a diet that is either entirely or primarily of plant origin (Morgan, 2019). As such, there is a growing research focus on the utilisation of plant proteins as novel food ingredients (Aschemann-Witzel et al., 2020).

Legumes are a rich source of plant protein. Legume-based protein is considered as one of the most promising alternatives to animal protein due to its abundance and relatively low cost (Can Karaca et al., 2015). Pea protein is primarily composed of globulins (55–80%) and albumins (18–25%). Among these two protein fractions, legumin (11S) and vicilin (7S) are the major types of protein in globulins (Fathi et al., 2018). Pea protein is rich in essential amino acids such as lysine and leucine, compared with soybean protein (Sánchez-Lozano et al., 2011; Xie et al., 2016). However, low solubility, low surface charge and a large number of hydrophobic residuals on the molecule surface of pea protein result in its poor functional properties, particularly solubility and emulsifying properties, thereby limiting its applications in food products (Karaca et al., 2011). To date, various physical, chemical and/or enzymatic methods have been developed and used to modify the functional properties of proteins (Kaushik et al., 2015; Pham et al., 2019; Weinbreck et al., 2003; Zha et al., 2019). Among these, protein-carbohydrate conjugation via Maillard reaction is the most straightforward and commonly used method. Maillard reaction usually occurs between the ε-amino group of lysine residues of proteins and the terminal reducing group of the carbonyl of carbohydrate (Martinez-Alvarenga et al., 2014). This reaction can significantly improve the solubility, thermal stability and emulsifying properties of protein (Oliveira et al., 2016; Zha et al., 2020).

Conventionally, Maillard reaction between a protein and a carbohydrate is commonly carried out using the dry-heating route. Briefly, protein and carbohydrate are mixed at a certain ratio and dissolved in water followed by drying of the mixture (e.g., using freeze-drying) to convert into mixture powder. This powder is subsequently incubated at the controlled temperature (mostly 60–70 °C) and relative humidity (mostly 65–79%) for certain days (1–14 days) to facilitate the Maillard reaction (Sedaghat Doost et al., 2019). Although this method works well at laboratory scale, its commercial application is challenging due to its

* Corresponding authors.
E-mail addresses: zijia.zhang@rmit.edu.au (Z. Zhang), benu.adhikari@rmit.edu.au (B. Adhikari).

https://doi.org/10.1016/j.fufo.2022.100193
Received 1 June 2022; Received in revised form 5 September 2022; Accepted 21 September 2022

long reaction time and the difficulty to control the degree or progress of reaction (Pirestani et al., 2017; Zhu et al., 2008).

The Maillard reaction when carried out via the wet-heating route is more promising because it maximises the contact between protein and carbohydrate molecules in the solution, thus, reducing the heating time. In wet-heating method, the mixture of protein and carbohydrate is dissolved in water and the mixture is heated at a set temperature and time to accelerate conjugation (Sedaghat Doost et al., 2019). In this method, the reaction time required for conjugation can be significantly reduced to few hours. This wet heating method of Maillard reaction is increasingly used to modify the functional properties of proteins (Pirestani et al., 2017; Wang et al., 2018; Wen et al., 2020; Zhang et al., 2014; Žilić et al., 2012).

Briefly, Maillard reaction can be divided into three stages. In the initial stage, Schiff base is formed due to the reaction between free amino groups of protein and reducing sugar of carbohydrate, which then convert into colourless Amadori compounds (Henle, 2005). The formation of Amadori compounds can be used as an indicator of the initial stage. When the reaction proceeds further, degradation of the intermediates occurs by condensation with free amino acids leading to the formation of Strecker aldehydes (Silván et al., 2006). The Amadori compounds undergo several degradation reactions at longer reaction time, known as advanced stage during which Advanced glycation end products (AGEs) such as pentosidine and N(ε)-Carboxymethyllysine are formed (Poulsen et al., 2013). The formation of brownish colour of "melanoidins" is used as the indicator of advanced stage of Maillard reaction. The AGEs have now been shown to be detrimental to human health. AGEs can result in oxidative stress and promote inflammatory processes causing chronic diabetes and cardiovascular diseases (Friedman, 2003). It is necessary to control the Maillard reaction within initial or intermediate stage to avoid the formation of AGEs.

However, to the best of our knowledge, most of the published research on Maillard reaction carried out through the wet-heating route are focused on the modification of protein structure and functional property. There is a paucity of research aimed at investigating the efficacy of Maillard reaction induced protein-polysaccharide conjugation at the initial stage when carried out using wet-heating route. The effect of this conjugation (wet heating route, first stage of Maillard reaction) on the functional properties of plant proteins is not systematically studied. Therefore, in this study, we used pea protein isolate (PPI) and maltodextrin (MD) as model plant protein and carbohydrate, respectively to induce Maillard reaction following the wet-heating route. The reaction was controlled at its initial stage and the effect of this conjugation on the protein's properties including solubility, molecular weight, secondary structure, and emulsifying properties was investigated. The outcome of this will provide greater insights on modification of structure-function of plant proteins through Maillard reaction, avoiding the reaction to proceed to advanced stage and applying the conjugates as sustainable emulsifiers.

2. Material and methods

2.1. Material

Pea protein isolate (PPI, NUTRALYS® S85 XF) and maltodextrin (MD) with a dextrose equiveillance of 39 (GLUCIDEX® 39) were provided by Roquette Pty Ltd. (Lestrem, France). The PPI contained 84.17% protein (Kjeldahl method, N × 6.25), 6.96% moisture (AOAC Method No. 925.10), 4.46% ash (AOAC Method No. 923.03), and 1.8% lipid (AOAC Method N0. 920.85). Commercial canola oil was purchased from the local market (Coles Pty Ltd., Victoria, Australia). All chemicals including sodium chloride, sodium hydrate, sodium dodecyl sulfate (SDS), 2 × Laemmli buffer, β-mercaptoethanol, Tris, glycine, bromophenol blue, Coomassie Brilliant Blue R-250, and Bradford assay reagents were of analytical grade and were purchased from Sigma-Aldrich Pty Ltd. (NSW, Australia).

2.2. Preparation of PPI-maltodextrin conjugates

In our preliminary experiments, PPI and MD were mixed at ratios of 2:1, 1:1, and 1:2 (w/w), respectively to induce the conjugation and the conjugates were dissolved in the water at the solid-to-water ratio of 1:7, 1:9 and 1:11 (w/w), respectively to produce oil-in-water emulsions. We found that the emulsion stabilized by the conjugate with PPI-to-MD ratio of 1:1 (w/w) and conjugate solid-to-water ratio of 1:9 (w/w) had the best stability. Therefore, these parameters were used to produce PPI-MD conjugate and its dispersion. Briefly, PPI and maltodextrin mixture (1:1, w/w) was added into Milli Q water (solid: water ratio = 1:9, w/w) and agitated (300 rpm) overnight at ambient temperature. Subsequently, the solution was adjusted to pH 7.5, 8.0 and 8.5 using 1M NaOH. These solutions were heated at 90 °C for up to 5 h using a shaking bath to induce Maillard reaction (protein-carbohydrate conjugation). Samples were collected for 5 h in 0.5 h intervals and freeze-dried (Freeze Dryer-VaCo 10, Australia) at 0.1 mBar and -80 °C for 48 h to prepare the powder product. These lyophilized samples were stored at 4 °C until further tests.

2.3. Detection of Amadori compounds and melanoidins

The progress of the Maillard reaction was determined according to Zha et al.(2019). Briefly, the ultraviolet-visible (UV) absorbance of the resulting conjugate was measured at 304 and 420 nm to indicate the formation of colourless Amadori compounds and brown melanoidins, respectively (Kutzli et al., 2020). The freeze-dried PPI-MD conjugate powder was dispersed in Milli Q water to prepare 1 mg/mL solution. Subsequently, the solution was transferred to quartz cuvettes (10 mm path length × 2 mm width × 45 mm height), and the measurements were made using a UV Spectrometer (Lambda 35, PerkinElmer., USA) with Milli Q water as the blank reference.

2.4. Measurement of colour parameters

The colour profile of the conjugate solution was determined using a chromameter (Minolta, CR-310, Japan), in terms of Commission Internationale de l'Eclairage (CIE) L^* (lightness), a^* (red/green intensity) and b^* (yellow/blue intensity) values. For the equipment calibration, a standard white tile (L^* = 97.1480, a^* = 5.2085, and b^* = -3.1112) was used.

2.5. Characterisation of PPI-MD conjugates

2.5.1. Molecular weight of PPI-MD conjugates

The molecular weight of PPI-MD conjugates as well as that of PPI was determined using sodium dodecyl sulfate-polyacrylamide gel electrophoresis (SDS-PAGE) under the reducing condition, according to Laemmli (1970)'s method. Briefly, a 4–15% precast polyacrylamide gel containing 4% stacking gel and 15% separation gel was applied in a Mini-PROTEAN Tetra Cell (Bio-Rad, Mini-Protein apparatus III). Four microliters of 5 mg/mL sample solution was mixed with 12 μL of 1 × phosphate buffer solution (pH 7.0) and 4 μL of loading buffer (95% 2 × Laemmli buffer and 5% β-mercaptoethanol) to make 1 μg/ μL solution, followed by heating samples at 100 °C for 10 min. Ten microliter sample was loaded into the precast gel and the electrophoresis was performed in a Tris-glycine running buffer (pH 8.3). The SDS-PAGE test was run at 110 V for 60–80 min until the dye front reached the reference line. After gel electrophoresis, the gel was stained with Coomassie Brilliant Blue R-250 dye and destained with a decolorization solution composed of 10% (v/v) methanol and 10% (v/v) acetic acid. In this study, the molecular weight of native PPI was also determined as a control.

2.5.2. Infrared (FTIR) spectroscopic measurement of the change of secondary structure

The FTIR spectra of PPI, MD, PPI-MD mixture and PPI-MD conjugates were determined using a Perkin Elmer Spectrum Two FTIR spectrometer

(Perkin Elmer, CT, USA) equipped with a Gladi ATR from Pike Technologies (Wisconsin, USA). The absorbance spectrum of air was used as background. The absorbance spectra of the test samples in the wavenumber range of 4000 to 400 cm^{-1} were recorded at a resolution of 1 cm^{-1} (64 scans).

The secondary structures (α-helix, β-sheet, β-turn and random coil) of PPI and PPI-maltodextrin conjugates were analysed using the method reported by Xu et al. (2019) with minor modification. Briefly, each FTIR spectrum in the wavenumber region of 1600–1700 cm^{-1} (amide I) was baseline corrected and smoothed using an 11-point Savitzky-Golay function to subtract the background noise. Each spectrum was deconvoluted by Fourier self-deconvolution method using the Ominic 8.2 software (Thermo Fisher Scientific, Carlsbad, USA). Origin 2016 software (OriginLab, Northampton, USA) was used to conduct the second-derivative analysis, and the deconvolution curve of amide I (1600–1700 cm^{-1}) band was fitted with Gaussian curve. Band of second derivatives of amide I commonly reflects the position of peaks of individual secondary structure, and the content of each structure can be calculated using the area under each sub peak (Ye et al., 2017).

2.5.3. Solubility of PPI-MD conjugates

The solubility of PPI-MD conjugates was determined using Bradford method (Bradford, 1976). Briefly, the freeze-dried PPI-MD conjugate powder was dispersed in Milli Q water to prepare 1 mg/mL solutions. The mixture was agitated for 30 min at ambient temperature to allow complete rehydration. Then, the pH of the mixture was adjusted to 3.0–8.0 using 1M HCl or NaOH as required. The pH-adjusted solution was centrifuged at 3000 × g for 15 min at 22 °C and the supernatant was collected. One hundred microlitres of this supernatant and 3 mL of Bradford assay solution were mixed and incubated at ambient temperature for 10 min. The absorbance of the incubated samples was measured at 595 nm using the UV–Vis spectrophotometer to calculate its protein content. Bovine serum albumin (BSA) was used as the standard to generate a standard curve. The solubility of PPI-MD conjugates was calculated using Eq. (1).

$$Solubility\ (\%) = \left(\frac{Ps}{Pt}\right) \times 100\% \tag{1}$$

where Ps is the protein content in the supernatant (mg/mL), Pt is the total protein content in the conjugate before centrifugation (mg/mL), measured by the Kjeldahl method ($N \times 6.25$). The solubility of PPI was also measured as a control.

2.5.4. Zeta-potential of PPI-MD conjugate

The above PPI-MD conjugate solution (1 mg/mL) was diluted by 10 times using Milli Q water and the pH of the diluted samples was adjusted within 3.0–8.0. These solutions were then centrifuged at 3000 × g for 15 min at 22 °C and the supernatants were collected. Zeta-potential of these supernatants was measured using a zeta sizer (Nano-ZS, Malvern Instruments Ltd., Malvern, UK). Zeta-potential values of PPI solution at the same concentration and pH were also determined as control.

2.6. Preparation of oil-in-water (O/W) emulsion and characterisation

2.6.1. Preparation of O/W emulsion

The PPI-MD conjugate powder was dissolved in Milli Q water at 1.0 and 2.0% (w/w) and the pH of the solution was adjusted to 7.0. Subsequently, canola oil was added to these solutions and the mixture was homogenised using a high shear homogeniser (IKA T25 Ultra Turrax, Wilmington, USA) at 15,000 rpm for 2 min. These preliminary emulsions were further homogenised using a Microfluidizer (M-110L Microfluidizer®, Microfluidics, Lampertheim, Germany) to produce fine O/W emulsions at 40 and 60 MPa, respectively using 3 passes. The oil content in the emulsion was controlled at 10% (v/v).

2.6.2. Droplet size and zeta-potential of O/W emulsion

The droplet size and zeta potential of freshly made O/W emulsion were measured using the zeta sizer at 25 °C. Briefly, to avoid multiple light scattering effects, the emulsions were diluted 100 times with 1% (w/w) sodium dodecyl sulfate (SDS) solution during particle size measurement. Milli Q water was used to dilute the emulsion by 100 times while measuring zeta potential.

2.6.3. Physical stability of the O/W emulsion

To evaluate the stability of emulsions, their emulsion stability index (ESI) was calculated based on the measurement of emulsion turbidity (Pearce and Kinsella, 1978). Briefly, the freshly made O/W emulsions (2%, w/w of protein concentration and homogenised at 60 MPa) were transferred into sealed glass test tubes and incubated in a pre-heated water bath for 6 h at different temperatures (25, 30, 40, 50 and 60 °C) to mimic potential thermal treatment during food production. After incubation, these emulsions were diluted by 100 times using 0.1% (w/w) SDS solution to the oil-volume fraction of 0.1% (v/v). The absorbance of the diluted samples at 500 nm was measured using the UV-Vis spectrometer and the turbidity of the emulsion was calculated using Eq. (2).

$$T = 2.303 \times \frac{A}{L} \times D \tag{2}$$

Where, T is the turbidity of emulsions in m^{-1}, A is the observed absorbance, D is the dilution factor (100 ×), and L is the pathlength of the cuvette (0.1 m).

The emulsion stability index (ESI, expressed in h) of emulsions was calculated using Eq. (3) (Sui et al., 2017)

$$ESI = \left(\frac{T_0}{T_0 - T}\right) \times t \tag{3}$$

Where, T_0 is the turbidity of fresh emulsion in m^{-1} determined immediately after it was prepared, T is the turbidity of the emulsion at the end of storage in m^{-1}, t is the time (6 h).

2.7. Statistical analysis

Experiments were carried out in triplicate unless mentioned otherwise. The results are expressed as mean ± standard deviation and the data analysis was performed using SPSS statistical software (SPSS 23.0, IBM, Armonk, NY, USA). Significant difference between any two mean values was made determined using one-way analysis of variance (ANOVA) by the Duncan test at 95% confidence level ($p < 0.05$).

3. Results and discussion

3.1. Colour change of PPI-MD conjugates during reaction

The absorbance values of PPI-MD conjugates at both 304 and 420 nm during Maillard reaction (conjugation) at different pH are presented in Fig. 1A and 1B, respectively. It is snow commonly accepted that, during the early stage of Maillard reaction, carbonyl group of a reducing sugar reacts with the ε-amino group of protein of which free lysine is the most reactive one (Hellwig and Henle, 2014; Ledl and Schleicher, 1990; Rooijen et al., 2013). Zhou et al. (2021) reported that the free lysine groups in pea protein isolate was 9.70 mg/g which is expected to readily react with the carbonyl group of carbohydrate in Maillard reaction. As shown in Fig. 1, the absorbance values of samples increased significantly with the increase of reaction time at both wavelengths, due to the continuous conjugation between PPI and MD. This is consistent with Zha et al. (2020)'s findings during the conjugation of PPI and gum Arabic. As shown in Fig. 1A, the absorbance of PPI-MD conjugate at 304 nm increased with the increase of pH value, suggesting more Amadori compounds were formed at the higher pH. A similar trend was also observed in the absorbance of conjugate at 420 nm, particularly when the reaction was performed at pH 8.5. This can be attributed to the acceleration of

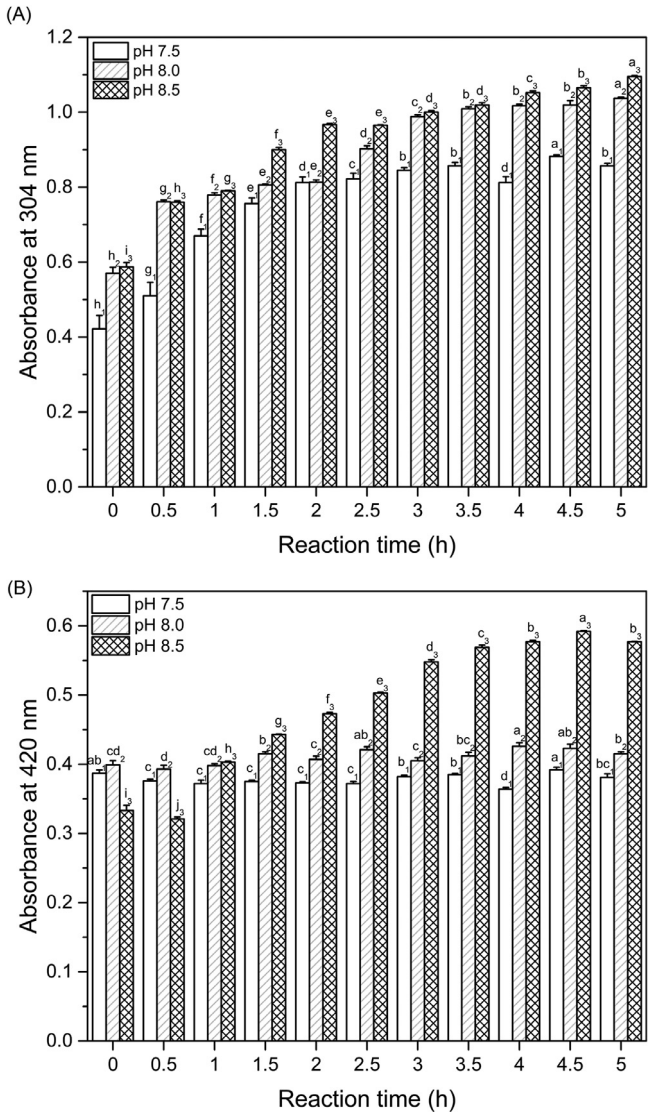

Fig. 1. Absorbance of different PPI-MD conjugates at (A) 304 nm and (B) 420 nm.

the Maillard reaction at higher pH conditions. The PPI used in this study had an isoelectric point (pI) around 4.4 (Fig. 5A). Therefore, the increase of pH above PPI's pI led to the unfolding and solubilisation of protein, which promoted the exposure of amino acids originally hidden in the hydrophobic core of protein structure. This enabled a higher number of free amino groups to react with the reducing groups of maltodextrin.

Interestingly, the absorbance of conjugate at 420 nm almost remained unchanged when the reaction was controlled at pH 7.5 and 8.0. The absorbance of conjugate at 420 nm of pH 8.5 continually increased with increase of reaction time, indicating the formation of brown coloured melanoidins. A similar phenomenon of change of absorbance of conjugate at 420 nm was observed from Lertittikul et al.'s (2007) study. In their study, when the initial pH of porcine plasma protein-glucose samples increased from 8 to 12, the absorbance (at 420 nm) of the resulting conjugates increased significantly after heating for 2 h. This indicated that the increase in pH of the system influenced the degree of Maillard reaction. In this study, when the reaction was performed at pH 7.5 and 8.0, a significant increase of absorbance of the conjugates at 304 nm was observed, while its absorbance at 420 nm almost remained unchanged, indicating that the conjugation (Maillard) reaction was successfully controlled within the initial stage.

The colour parameters (L^*, a^* and b^*) of the PPI-MD conjugates at three different pH are presented in Fig. 2A, 2B and 2C, respectively. During the reaction, the L^* value of the conjugates decreased gradually, while a^* and b^* values increased with the increase of reaction time. This trend was clearer at the higher pH. This result agrees well with the above absorbance data (Fig. 1), indicating the progress of conjugation with the increase of reaction time and the acceleration of the Maillard reaction at higher pH. A similar trend of colour change was reported by Zha et al. (2019).

It is worth noting that at pH 8.5, dark conjugates with undesirable odour were formed after 5 h reaction, indicating that the Maillard reaction had reached to the advanced stage. A similar phenomenon was reported in Wei et al. (2019)'s study, where glycation between flaxseed protein and D-xylose was performed. These authors detected the increased amount of undesirable flavour compounds, including ketones, furans and aromatics when the pH of the reaction was increased from 6.0 to 8.0. This was due to the fact that Amadori degradation was promoted at a high pH value. This observation further confirmed the fact that the reaction was confined within initial stage at pH 7.5 and 8.0. Based on this distinct colour change of PPI-MD conjugate at pH 8.5, pH 8.0 was selected as the optimum pH to achieve a higher Maillard reaction rate while at the same time controlling the reaction at the initial stage.

3.2. Molecular weight change of PPI-MD conjugates during reaction

The molecular weight change of PPI during the conjugation is shown in Fig. 3. Several molecular weight bands were observed in the native PPI within 15–75 kDa. Particularly, the bands observed at 28.7, 33.3 and 47.3 kDa indicated by vicilin, 22.3–23.1 kDa indicated 11S legumin and 72.4–77.9 kDa indicated by conviclin fractions, respectively (Zhao et al., 2022). No molecular weight band was observed in lane 2, which is expected as the molecular weight of maltodextrin MD was well below the lowest value in the marker scale (< 10 kDa) (Zhang et al., 2014). As shown in lane 3, no significant change of the molecular weight was observed in the PPI-MD mixture, compared to that of PPI which is also expected as there is no likelihood of conjugation reaction occurring in the mixture without heating and at neutral pH. After the Maillard reaction, new bands with high molecular weight beyond 250 kDa were observed in the PPI-maltodextrin conjugates (lane 4 and 5). Interestingly, some protein fractions in the PPI, particularly the ones with molecular weight in the range of 37–50 and 75–100 kDa, disappeared during the conjugation due to covalent bonding with MD (Zhao et al., 2022). Compared with PPI-MD conjugates obtained at 2.5 h of reaction, a high proportion of PPI-MD conjugates obtained at 5 h had a relatively high molecular weight (>250 kDa) than those with low molecular weight (20 to 100 kDa). This is due to higher extent of Maillard reaction induced conjugation at 5 h.

3.3. Changes in secondary structure of PPI due to conjugation

The FTIR spectra of native PPI, MD, PPI-MD mixture (0 h) and PPI-MD conjugates reacted for 2.5 and 5 h are shown in Fig. 4. In general, PPI exhibited the following characteristic peaks: C=O stretching at 1634 cm^{-1} (amide I), N-H bending at 1526 cm^{-1} (amide II), and C-N stretching and N-H deformation at 1394 & 1240 cm^{-1} (amide III) (Xu et al., 2019). The bands at 2975 & 2899 cm^{-1} were due to stretching of C-H in CH_2 and CH_3 groups (Zha et al., 2019). On the other hand, MD had a peak at 1069 cm^{-1}, contributed by the stretching of C-C and C-O and the C-H bending (Wang et al., 2013). In PPI-MD conjugates, increased intensity of C=O stretching, C-N stretching and C-O stretching was observed at 1634, 1394 and 1069 cm^{-1}, respectively when compared with the spectra of the native PPI and PPI-MD mixture. This can be attributed to the formation of Maillard reaction products such as Amadori compounds (C=O), Schiff base (C=N) and

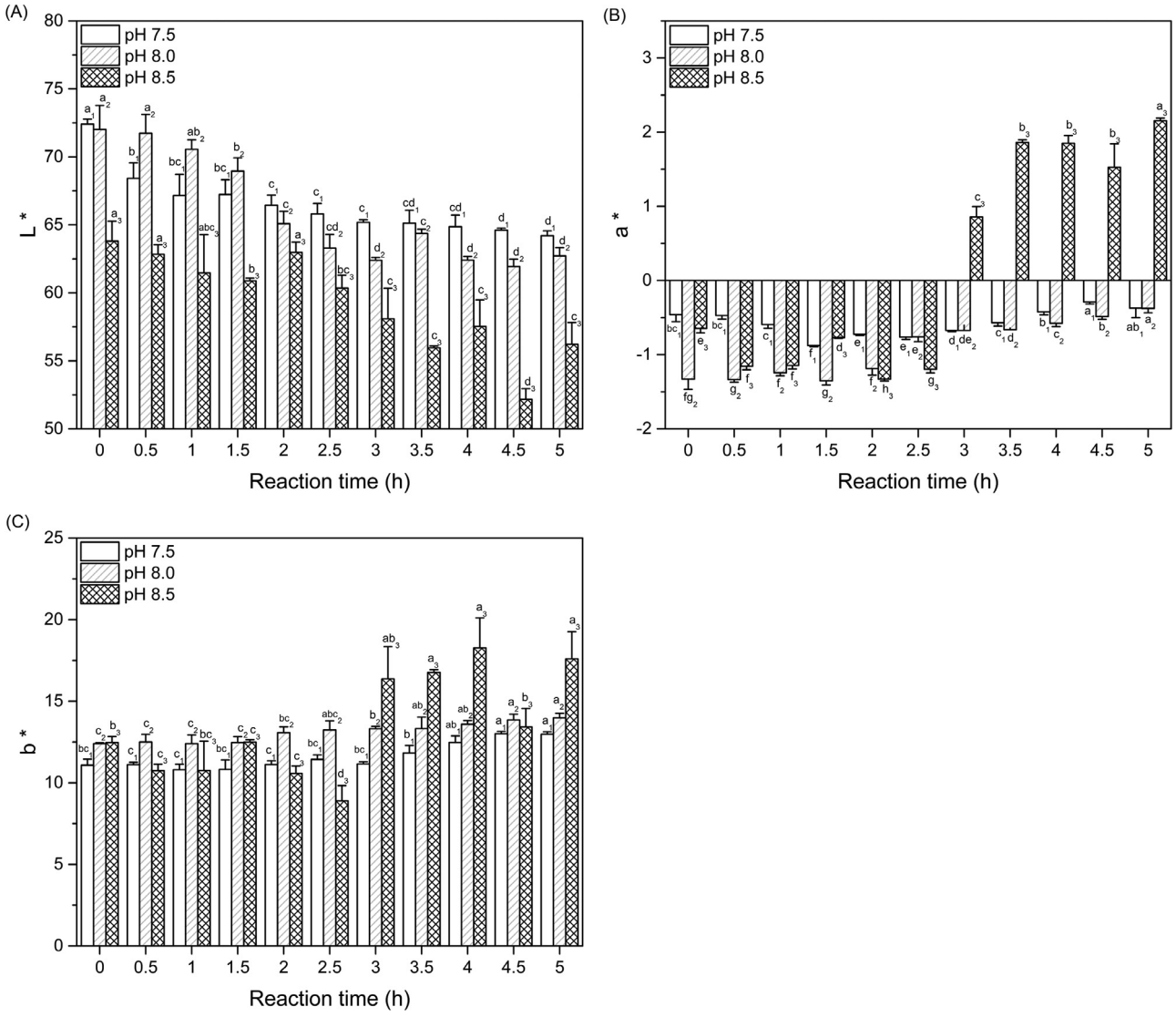

Fig. 2. Colour profile and image of PPI-MD conjugates: (A) L* value; (B) a* value; (C) b*value.

Table 1
Composition of secondary structures of PPI, PPI-MD mixture and PPI-MD conjugates.

Sample	α-helix	ß-sheet	ß-turns	Random coil
PPI	41.6 ± 1.5^{a}	28.4 ± 1.9^{a}	14.5 ± 2.5^{a}	15.6 ± 1.0^{a}
PPI-MD 0 h	42.7 ± 1.0^{a}	26.1 ± 0.7^{a}	8.9 ± 0.8^{b}	22.4 ± 0.9^{b}
PPI-MD conjugate 2.5 h	45.5 ± 0.3^{b}	23.8 ± 1.6^{b}	6.7 ± 1.1^{b}	24.0 ± 1.4^{b}
PPI-MD conjugate 5 h	46.4 ± 0.12^{b}	21.9 ± 1.1^{c}	5.3 ± 0.7^{c}	26.4 ± 1.0^{c}

The different letters in superscript within a column indicate statistically significant differences ($p < 0.05$) with in the group.

pyrazines (C-N) through covalent bonding between PPI and maltodextrin (Srivastava et al., 2011). A further increase of intensity in above-mentioned peaks was observed in PPI-MD conjugates when reaction was carried out for 5 h due to increased grafting or conjugation between PPI and MD.

The composition of secondary structural features of PPI, PPI-MD mixture and PPI-MD conjugates deduced from the FTIR spectra are presented in Table 1. PPI had approximately 41.6 ± 1.5% α-helix, 28.4 ± 1.9% β-sheet, 14.5 ± 2.5% β-turns and 15.6 ± 1.0% random coil. No significant difference ($p > 0.05$) was found in the composition of α-helix and β-sheet contents between the native PPI and PPI-MD mixture. Interestingly, the percent composition of β-turn and random coil increased significantly in PPI-MD mixture compared to that in native PPI. This can be due to the formation of hydrogen bonds between PPI and MD molecules in the aqueous solution and when this mixture was dried increased β-turn and random coil content (Shang et al., 2020). When conjugated for 2.5 h, compared with native PPI, the α-helix and random coil content of the conjugates increased significantly, while the content of β-sheet and β-turn decreased. This indicates the change of spatial structure of PPI caused by conjugation. The β-sheet structure in protein usually has a relatively large surface area, which facilitates the formation of hydrogen bonds between protein molecules. However,

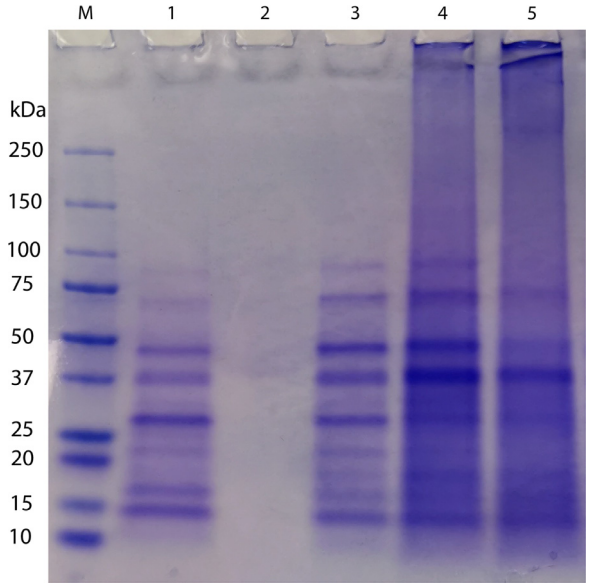

Fig. 3. Molecular weight of PPI and PPI-maltodextrin (MD) conjugates: Lane M for protein marker, lane 1 for PPI, lane 2 for MD, lane 3 for PPI-MD mixture, lane 4 for PPI-MD conjugate heating for 2.5 h, lane 4 for PPI-MD conjugate heating for 5 h.

the presence of carbohydrates in the system prevented the interaction between protein molecules, resulting in a decrease in β-sheet content and an increase in random coil content (Liu et al., 2021). Furthermore, thermal treatment promoted the unfolding of protein molecules, leading to the formation of disordered random coil structures (Ngarize et al., 2004).

A further increase in random coil and decrease in β-sheet and β-turns contents were observed in the conjugates when the heating time was longer (5 h in this case). It is worth noting that the increased random coil content in PPI-MD conjugates suggests a more flexible structure and it is expected to improve the emulsifying properties (Chen et al., 2019).

3.4. Effect of conjugation on protein solubility

The solubility of PPI and PPI-MD conjugate in the pH range of 3.0–8.0 is shown in Fig. 5A. PPI exhibited its lowest solubility of 2.81 ± 0.02% (w/w) at pH 4.4, which is its isoelectric point (Fig. 5B). After conjugation with MD, the solubility of PPI increased significantly in the tested pH range. Particularly, the solubility of protein increased by 2-3 fold between pH 4.0 and 5.0. This level of increase in pH of PPI, particularly at a low solubility range, is due to the conjugation (attachment) of more water-soluble MD to the protein molecular chain via covalent bonds, thereby improving the affinity of the PPI-MD conjugates with water molecules (Oliveira et al., 2016). As mentioned in Section 3.1, the increase of pH above PPI's pI resulted in the unfolding of protein structure, which is conducive for the progress of Maillard reaction between PPI and MD and thus increasing the solubility of protein (Cheng et al., 2022). In addition, the solubility of PPI-MD conjugates increased significantly as the reaction time increased from 2.5 to 5 h due to a higher level of conjugation. The level of increase of PPI solubility after conjugation with MD can be due to less availability of hydrophobic amino acids, particularly cysteine and isoleucine. During Maillard reaction cysteine and isoleucine participate in the covalent bonding with reducing groups of carbohydrate (Hemmler et al., 2018). Therefore, the conjugation between PPI and MD reduces the available cysteine and isoleucine content in PPI ultimately increasing its solubility.

3.5. Effect of conjugation on surface charge

The Zeta-potential values of PPI and the PPI-MD conjugates reacted for 2.5 and 5 h are shown in Fig. 5B in the pH range of 3.0–8.0. As shown, PPI was neutral at pH 4.4 (pI) and this agrees well with its lowest solubility in Fig. 5A. After conjugation, the PPI-MD conjugates became substantially more negatively below PPI's pI and less positively charged above the pI. This is because the positively charged amino acids, particularly lysine, conjugated with negatively charged MD, leading to the formation of more negatively charged conjugates (Wang et al., 2018). As a result, the pI of PPI-MD conjugates shifted toward the lower pH range after conjugation. Previous study on conjugation between whey protein isolate and inulin also showed that the zeta-potential of WPI-inulin conjugate (after wet-heating at 70 °C for 2 h) had larger surface

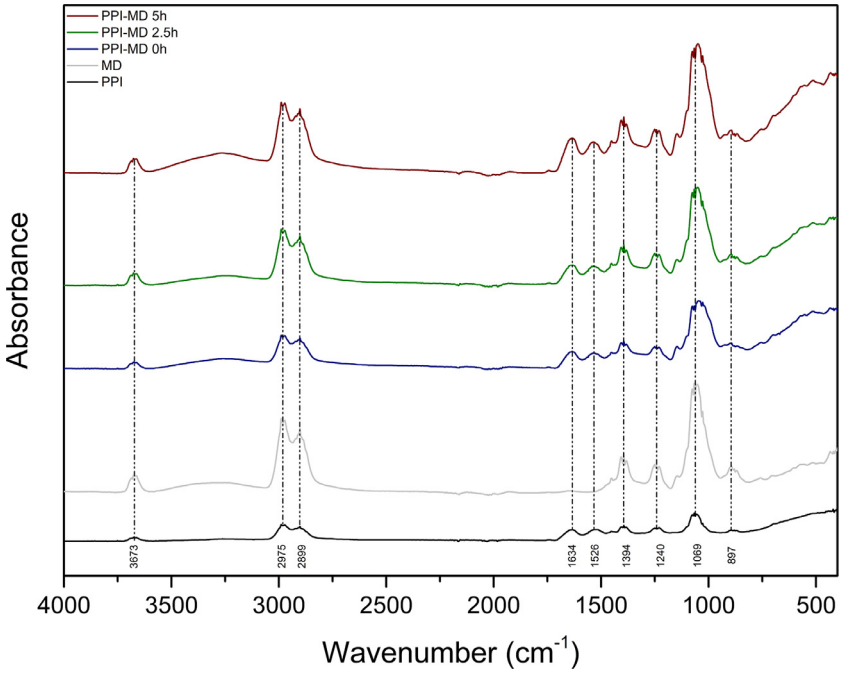

Fig. 4. FTIR spectra of PPI, MD, PPI-MD mixture and PPI-MD conjugates obtained at 2.5 and 5 h, respectively.

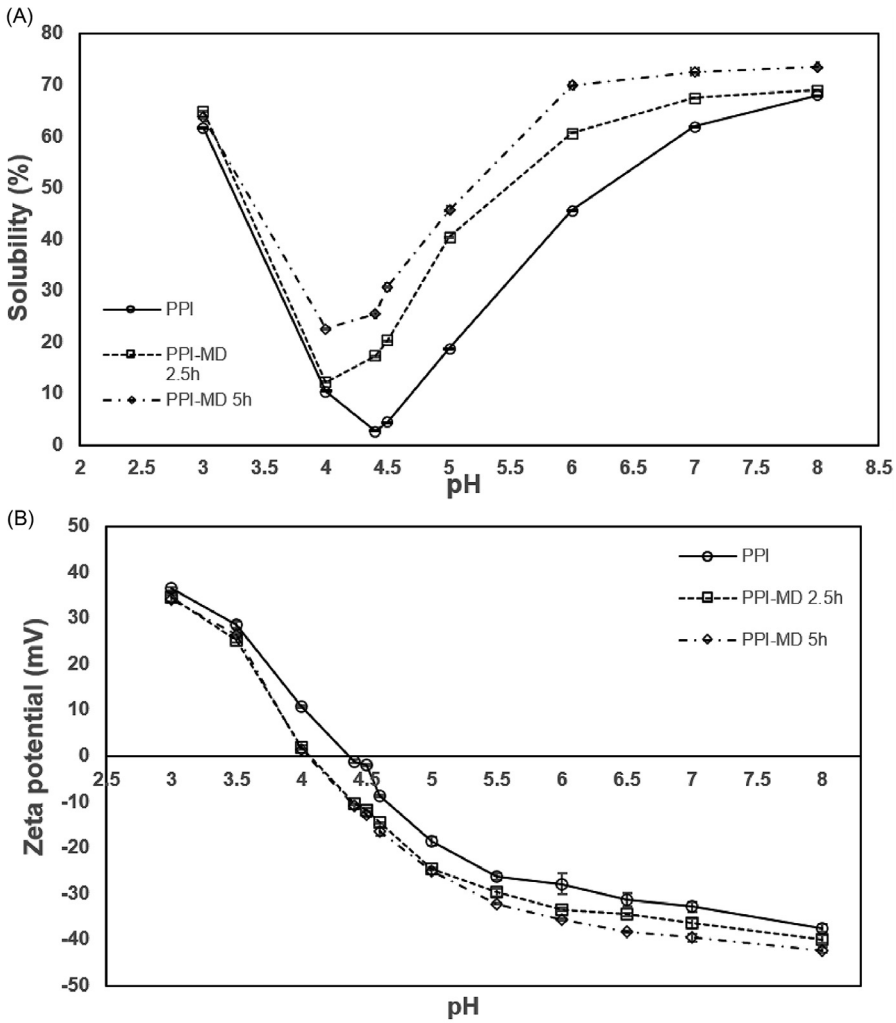

Fig. 5. Solubility and Zeta-potential of PPI and PPI-MD conjugates as a function of pH: (A) Solubility and (B) Zeta-potential.

charge than native WPI (Wang et al., 2020). Higher surface charge of these conjugate indicated to their better capacity to stabilise oil droplets in emulsion.

3.6. Characteristics of oil-in-water (O/W) emulsions

3.6.1. Droplet size of O/W emulsions stabilised by PPI-MD conjugates

Z-average diameter of oil-in-water (O/W) emulsions stabilised by PPI and PPI-MD conjugate at two emulsifier concentrations (1% and 2%, w/w) prepared at different homogenisation pressures (40 and 60 MPa) is shown in Fig. 6. At both homogenisation pressures, and at a fixed emulsifier concentration, the conjugate-stabilised O/W emulsion exhibited a significantly smaller size than the one stabilised by PPI. This indicates the improved emulsifying property of PPI-MD conjugates, compared to PPI. Also, emulsions with a decreased diameter were formed when conjugates produced at higher conjugation time were used. This is most probably due to the improved interfacial activity and interface resilience of the conjugates compared to PPI (Zhang et al., 2012). It is also expected that higher solubility and flexibility of a protein make it a better emulsifier (Shevkani et al., 2015). A protein with higher solubility can be easily dissolved and it can easily migrate to the oil/water interface and gets adsorbed there in a shorter time (Shevkani et al., 2019). Mozafarpour et al. (2019) reported that the O/W emulsion stabilised by protein with a higher random coil content had a lower droplet size. This is because this flexible structure enabled it to absorb and reorient at the oil/water interface rapidly and, thus, decrease the droplet size. As discussed in Sections 3.3 and 3.4, PPI-MD conjugation increased the random coil content and resulted in a more flexible structure and improved protein solubility. This is expected to enhance the adsorption efficiency of PPI-MD conjugate at the oil/water interface. The droplet size of the O/W emulsion stabilised by PPI-MD conjugates and PPI decreased significantly with the increase of emulsifier content (Fig. 6A and 6B). Higher number of PPI or PPI-MD molecules was expected to adsorb at the oil-water interface and stabilise the emulsion when their content was increased (Kasran et al., 2013).

3.6.2. Impact of conjugation on zeta potential and emulsion droplet size

The Zeta-potential of O/W emulsion droplets stabilised by PPI and PPI-MD conjugates is presented in Fig. 6C and 6D. No significant difference was observed when comparing the Zeta-potential of emulsion droplets stabilised by PPI and PPI-MD conjugate obtained at 2.5 h at 1% (w/w) emulsifier concentration. This observation suggested that the PPI and PPI-MD 2.5 h conjugate exhibited similar emulsifying properties at this concentration, despite PPI-MD conjugate having higher negative charge than PPI at given pH (pH = 7.0). This may be due to low steric hindrance offered by the PPI-MD 2.5 h conjugate as the degree of conjugation was low (Ng et al., 2017). This is also due to low emulsifier concentration (PPI or PPI-MD 2.5 h conjugate). When the emulsifier concentration increased to 2% (w/w), the magnitude of the zeta-potential of the emulsions stabilised by conjugates increased significantly, indicating the electrostatic repulsive force was stronger. The emulsion droplets stabilised by conjugates produced at 5 h had higher

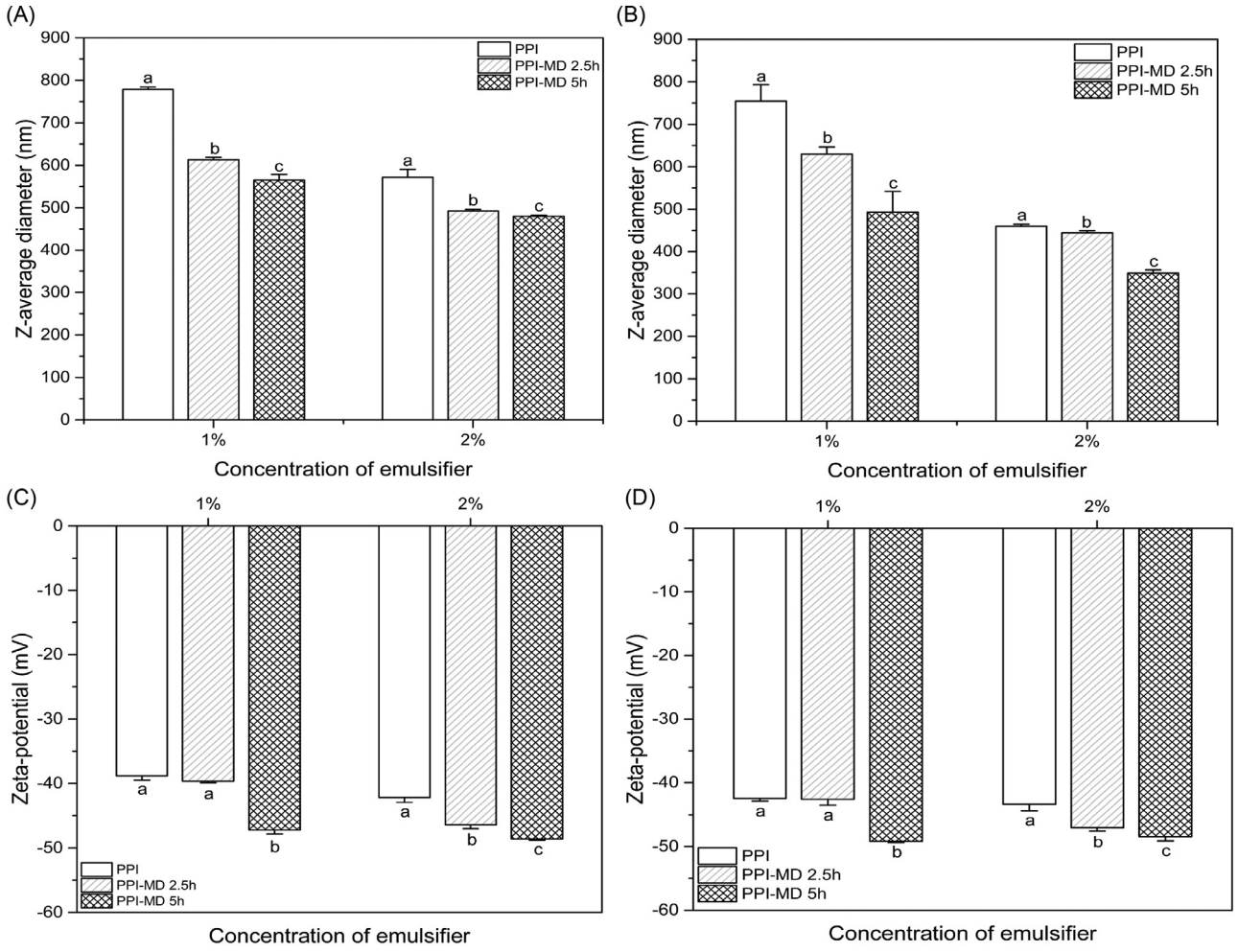

Fig. 6. Characteristics of O/W emulsions stabilised by PPI and PPI-MD conjugates: (A) Droplet size, homogenised under 40 MPa; (B) Droplet size, homogenised under 60 MPa; (C) Zeta-potential, homogenised under 40 MPa; (D) Zeta-potential, homogenised under 60 MPa.

negative change than the ones stabilized by conjugates produced at 2.5 h of reaction. The PPI-MD conjugated produced at 5 h of reaction tended to form an emulsion with smaller droplet size (Fig. 5B), compared to the conjugated produced at 2.5 h of reaction. This can be attributed to their favourable adsorption at the O/W interface. This would increase the thickness of the interfacial layer and would promote the stability of emulsion (Dickinson, 2009).

3.6.3. *Physical stability of O/W emulsions stabilised by PPI-MD conjugates*

The emulsion stability (in terms of emulsion stability index, ESI) of O/W emulsion produced using PPI and PPI-MD conjugates produced at 2.5 and 5 h is presented in Fig. 7 at four temperatures. At a particular storage temperature, the ESI of the emulsion stabilised by PPI-MD conjugates was significantly higher than the one stabilised by PPI. The ESI of emulsion stabilised by PPI-MD conjugated produced at 5 h of reaction was also significantly higher than those produced using PPI-MD conjugate produced at 2.5 h of reaction in each temperature. A similar trend was also observed by Chen et al. (2019) in the case of soybean oil stabilised O/W emulsion using whey protein isolate (WPI) and WPI-gum Acaia (GA) conjugate as emulsifiers. These authors reported a significant improvement of ESI of WPI-GA conjugates as compared with WPI, and the ESI of conjugates further increased with higher glycation degree (DG value). This improved stability can be attributed to the decreased O/W emulsion droplet size (Section 3.7.1), increased repulsive electrostatic force (zeta potential) of the droplets (Section 3.7.2) and improved steric hindrance offered by the PPI-MD conjugates (Zhang et al., 2012). All the emulsions exhibited a decreased ESI with the increase of

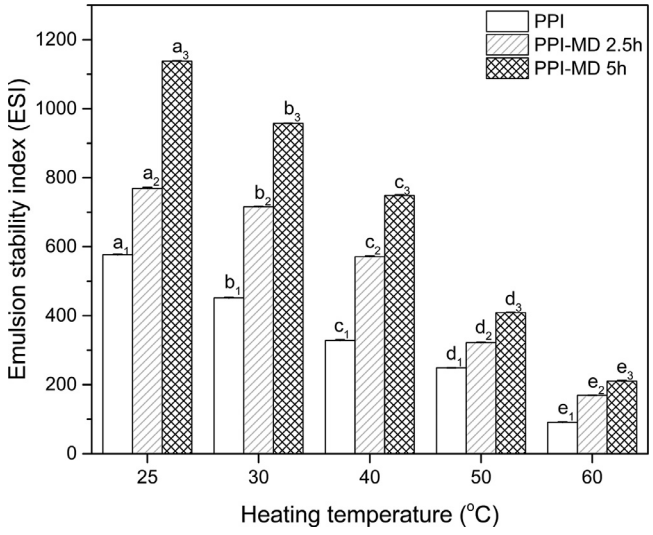

Fig. 7. Emulsion stability index (ESI) of emulsion stabilised PPI and PPI-maltodextrin conjugates as a function of temperature.

storage temperature, which can be attributed to the unfolding of protein anchored on the O/W interface at higher temperature, disruption of the interfacial layer due to the mobility of the emulsifiers and decrease of surface charge of PPI as well as PPI-MD conjugates. A simi-

lar trend on temperature-induced emulsion instability was observed by Jiang et al. (2022) in pea protein-inulin conjugate. The emulsion stabilised by this conjugate showed an increase of droplet size and flocculation when the temperature increased to 90 °C, which was attributed to temperature-induced aggregation. Overall, the O/W emulsion stabilised by PPI-MD conjugate exhibited high ESI values up to 60 °C. This indicates that PPI-MD conjugate produces more stable emulsions during food processing.

4. Conclusion

Conjugation between PPI and MD was carried out at 90 °C following the wet-heating route of Maillard reaction. The Maillard reaction was controlled within the initial stage by controlling pH, temperature, and time of reaction. Increase of pH and time were, in general, conducive for Maillard reaction induced conjugation. The PPI-MD conjugation remained within the initial stage at pH 7.5 and 8.0 and time up to 5 h as no significant melanonids were formed. MD was successfully conjugated with PPI as indicated by the increase of molecular weight. The random coil content in PPI-MD conjugates increased significantly making them better emulsifiers. The functional properties of PPI were improved significantly after conjugation. The solubility of PPI-MD conjugates was significantly higher than that of PPI. The PPI-MD conjugates acquired significantly higher negative charges compared to PPI. The O/W emulsion stabilised by PPI-MD conjugates had smaller droplet size and higher magnitude of zeta-potential, compared to that stabilised by PPI, indicating improved emulsifying properties. The O/W emulsion stabilised by PPI-MD conjugate produced at 5 h reaction had ESI higher than 210 h at 60 °C. The controlled Maillard reaction carried out through the wet-heating route is a facile method that can be used to develop effective food-grade emulsifiers.

Ethical statement

Hereby, I (Zijia Zhang) consciously assure that for the manuscript "Maillard reaction between pea protein isolate and maltodextrin via wet heating route for emulsion stabilisation" the following is fulfilled:

Declaration of Competing Interest

The authors declare that they have no known competing financial interests or personal relationships that could have appeared to influence the work reported in this paper.

CRediT authorship contribution statement

Zijia Zhang: Conceptualization, Methodology, Writing – original draft. **Bo Wang:** Conceptualization, Supervision, Writing – review & editing. **Benu Adhikari:** Conceptualization, Supervision, Writing – review & editing.

Data Availability

Data will be made available on request.

References

Aschemann-Witzel, J., Gantriis, R.F., Fraga, P., Perez-Cueto, F.J.A., 2020. Plant-based food and protein trend from a business perspective: markets, consumers, and the challenges and opportunities in the future. Crit. Rev. Food Sci. Nutr. 0 (0), 1–10. doi:10.1080/10408398.2020.1793730.

Bradford, M.M., 1976. A rapid and sensitive method for the quantitation of microgram quantities of protein utilizing the principle of protein-dye binding. Anal. Biochem. 72 (1), 248–254. doi:10.1016/0003-2697(76)90527-3.

Can Karaca, A., Low, N.H., Nickerson, M.T., 2015. Potential use of plant proteins in the microencapsulation of lipophilic materials in foods. Trends Food Sci. Technol. 42 (1), 5–12. doi:10.1016/j.tifs.2014.11.002.

Chen, W., Ma, X., Wang, W., Lv, R., Guo, M., Ding, T., … Liu, D., 2019. Preparation of modified whey protein isolate with gum acacia by ultrasound maillard reaction. Food Hydrocolloids 95, 298–307. doi:10.1016/j.foodhyd.2018.10.030.

Cheng, Y.H., Mu, D.C., Feng, Y.Y., Xu, Z., Wen, L., Chen, M.L., Ye, J., 2022. Glycosylation of rice protein with dextran via the Maillard reaction in a macromolecular crowding condition to improve solubility. J. Cereal Sci. 103, 103374. doi:10.1016/j.jcs.2021.103374.

Dickinson, E., 2009. Hydrocolloids as emulsifiers and emulsion stabilizers. Food Hydrocolloids 23 (6), 1473–1482. doi:10.1016/j.foodhyd.2008.08.005.

Fathi, M., Donsi, F., McClements, D.J., 2018. Protein-based delivery systems for the nanoencapsulation of food ingredients. Compr. Rev. Food Sci. Food. Saf. 17 (4), 920–936. doi:10.1111/1541-4337.12360.

Friedman, M., 2003. Chemistry, biochemistry, and safety of acrylamide. J. Agric. Food Chem. 51 (16), 4504–4526. doi:10.1021/jf030204.

Hellwig, M., Henle, T., 2014. Baking, ageing, diabetes: a short history of the Maillard reaction. Angew. Chem. Int. Ed. 53 (39), 10316–10329. doi:10.1002/anie.201308808.

Hemmler, D., Roullier-Gall, C., Marshall, J.W., Rychlik, M., Taylor, A.J., Schmitt-Kopplin, P., 2018. Insights into the chemistry of non-enzymatic browning reactions in different ribose-amino acid model systems. Sci. Rep. 8 (1), 16879. doi:10.1038/s41598-018-34335-5.

Henle, T., 2005. Protein-bound advanced glycation endproducts (AGEs) as bioactive amino acid derivatives in foods. Amino Acids 29 (4), 313–322. doi:10.1007/s00726-005-0200-2.

Jiang, W., Zhang, Y., Julian McClements, D., Liu, F., Liu, X., 2022. Impact of pea protein-inulin conjugates prepared via the Maillard reaction using a combination of ultrasound and pH-shift treatments on physical and oxidative stability of algae oil emulsions. Food Res. Int. 156, 111161. doi:10.1016/j.foodres.2022.111161.

Karaca, A.C., Low, N., Nickerson, M., 2011. Emulsifying properties of chickpea, faba bean, lentil and pea proteins produced by isoelectric precipitation and salt extraction. Food Res. Int. 44 (9), 2742–2750. doi:10.1016/j.foodres.2011.06.012.

Kasran, M., Cui, S.W., Goff, H.D., 2013. Covalent attachment of fenugreek gum to soy whey protein isolate through natural Maillard reaction for improved emulsion stability. Food Hydrocolloids 30 (2), 552–558. doi:10.1016/j.foodhyd.2012.08.004.

Kaushik, P., Dowling, K., Barrow, C.J., Adhikari, B., 2015. Complex coacervation between flaxseed protein isolate and flaxseed gum. Food Res. Int. 72, 91–97. doi:10.1016/j.foodres.2015.03.046.

Kutzli, I., Griener, D., Gibis, M., Schmid, C., Dawid, C., Baier, S.K., … Weiss, J., 2020. Influence of Maillard reaction conditions on the formation and solubility of pea protein isolate-maltodextrin conjugates in electrospun fibers. Food Hydrocolloids 101, 105535. doi:10.1016/j.foodhyd.2019.105535.

Laemmli, U.K., 1970. Cleavage of structural proteins during the assembly of the head of bacteriophage T4. Nature 227 (5259), 680–685. doi:10.1038/227680a0.

Ledl, F., Schleicher, E., 1990. New aspects of the Maillard reaction in foods and in the human body. Angew. Chem. Int. Ed. Engl. 29 (6), 565–594. doi:10.1002/anie.199005653.

Lertittikul, W., Benjakul, S., Tanaka, M., 2007. Characteristics and antioxidative activity of Maillard reaction products from a porcine plasma protein–glucose model system as influenced by pH. Food Chem. 100 (2), 669–677. doi:10.1016/j.foodchem.2005.09.085.

Liu, X., Yang, Q., Yang, M., Du, Z., Wei, C., Zhang, T., … Liu, J., 2021. Ultrasound-assisted Maillard reaction of ovalbumin/xylose: the enhancement of functional properties and its mechanism. Ultrason. Sonochem. 73, 105477. doi:10.1016/j.ultsonch.2021.105477.

Martinez-Alvarenga, M.S., Martinez-Rodriguez, E.Y., Garcia-Amezquita, L.E., Olivas, G.I., Zamudio-Flores, P.B., Acosta-Muniz, C.H., Sepulveda, D.R., 2014. Effect of Maillard reaction conditions on the degree of glycation and functional properties of whey protein isolate – maltodextrin conjugates. Food Hydrocolloids 38, 110–118. doi:10.1016/j.foodhyd.2013.11.006.

Mozafarpour, R., Koocheki, A., Milani, E., Varidi, M., 2019. Extruded soy protein as a novel emulsifier: structure, interfacial activity and emulsifying property. Food Hydrocolloids 93, 361–373. doi:10.1016/j.foodhyd.2019.02.036.

Ng, S.K., Nyam, K.L., Lai, O.M., Nehdi, I.A., Chong, G.H., Tan, C.P., 2017. Development of a palm olein oil-in-water (o/w) emulsion stabilized by a whey protein isolate nanofibrils-alginate complex. LWT Food Sci. Technol. 82, 311–317. doi:10.1016/j.lwt.2017.04.050.

Ngarize, S., Herman, H., Adams, A., Howell, N., 2004. Comparison of changes in the secondary structure of unheated, heated, and high-pressure-treated β-lactoglobulin and ovalbumin proteins using Fourier transform Raman spectroscopy and self-deconvolution. J. Agric. Food Chem. 52 (21), 6470–6477. doi:10.1021/jf030649y.

de Oliveira, F.C., dos Coimbra, J.S.R., de Oliveira, E.B., Zuñiga, A.D.G., Rojas, E.E.G., 2016. Food protein-polysaccharide conjugates obtained via the Maillard reaction: a review. Crit. Rev. Food Sci. Nutr. 56 (7), 1108–1125. doi:10.1080/10408398.2012.755669.

Pearce, K.N., Kinsella, J.E., 1978. Emulsifying properties of proteins: evaluation of a turbidimetric technique. J. Agric. Food Chem. 26 (3), 716–723. doi:10.1021/jf60217a041.

Pham, L.B., Wang, B., Zisu, B., Adhikari, B., 2019. Complexation between flaxseed protein isolate and phenolic compounds: effects on interfacial, emulsifying and antioxidant properties of emulsions. Food Hydrocolloids 94, 20–29. doi:10.1016/j.foodhyd.2019.03.007.

Pirestani, S., Nasirpour, A., Keramat, J., Desobry, S., 2017. Preparation of chemically modified canola protein isolate with gum Arabic by means of Maillard reaction under wet-heating conditions. Carbohydr. Polym. 155, 201–207. doi:10.1016/j.carbpol.2016.08.054.

Poulsen, M.W., Hedegaard, R.V., Andersen, J.M., de Courten, B., Bügel, S., Nielsen, J., … Dragsted, L.O., 2013. Advanced glycation endproducts in food and their effects on health. Food Chem. Toxicol. 60, 10–37. doi:10.1016/j.fct.2013.06.052.

van Rooijen, C., Bosch, G., van der Poel, A.F.B., Wierenga, P.A., Alexander, L., Hendriks, W.H., 2013. The Maillard reaction and pet food processing: effects on

nutritive value and pet health. Nutr. Res. Rev. 26 (2), 130–148. doi:10.1017/S0954422413000103.

R. Morgan, 2019. Rise in vegetarianism not halting the march of obesity. http://www.roymorgan.com/findings/7944-vegetarianism-in-2018-april-2018-201904120608

Sánchez-Lozano, N.B., Martínez-Llorens, S., Tomás-Vidal, A., Cerdá, M.J., 2011. Amino acid retention of gilthead sea bream (Sparus aurata, L.) fed with pea protein concentrate. Aquacult. Nutr. 17 (2), e604–e614. doi:10.1111/j.1365-2095.2010.00803.x.

Sedaghat Doost, A., Nikbakht Nasrabadi, M., Wu, J., A'yun, Q., Van der Meeren, P., 2019. Maillard conjugation as an approach to improve whey proteins functionality: a review of conventional and novel preparation techniques. Trends Food Sci. Technol. 91, 1–11. doi:10.1016/j.tifs.2019.06.011.

Shang, J., Zhong, F., Zhu, S., Wang, J., Huang, D., Li, Y., 2020. Structure and physiochemical characteristics of whey protein isolate conjugated with xylose through Maillard reaction at different degrees. Arab. J. Chem. 13 (11), 8051–8059. doi:10.1016/j.arabjc.2020.09.034.

Shevkani, K., Singh, N., Kaur, A., Rana, J.C., 2015. Structural and functional characterization of kidney bean and field pea protein isolates: a comparative study. Food Hydrocolloids 43, 679–689. doi:10.1016/j.foodhyd.2014.07.024.

Silván, J.M., van de Lagemaat, J., Olano, A., del Castillo, M.D., 2006. Analysis and biological properties of amino acid derivates formed by Maillard reaction in foods. J. Pharm. Biomed. Anal. 41 (5), 1543–1551. doi:10.1016/j.jpba.2006.04.004.

Srivastava, A.K., Iconomidou, V.A., Chryssikos, G.D., Gionis, V., Kumar, K., Hamodrakas, S.J., 2011. Secondary structure of chorion proteins of the Lepidoptera Pericallia ricini and Ariadne merione by ATR FT-IR and micro-Raman spectroscopy. Int. J. Biol. Macromol. 49 (3), 317–322. doi:10.1016/j.ijbiomac.2011.05.006.

Sui, X., Bi, S., Qi, B., Wang, Z., Zhang, M., Li, Y., Jiang, L., 2017. Impact of ultrasonic treatment on an emulsion system stabilized with soybean protein isolate and lecithin: Its emulsifying property and emulsion stability. Food Hydrocolloids 63, 727–734. doi:10.1016/j.foodhyd.2016.10.024.

United Nations, Department of Economic and Social Affairs, & Population Division. (2019). World population prospects highlights, 2019 revision Highlights, 2019 revision. https://population.un.org/wpp/publications/files/wpp2019_highlights.pdf

Wang, L.H., Sun, X., Huang, G.Q., Xiao, J.X., 2018. Conjugation of soybean protein isolate with xylose/fructose through wet-heating Maillard reaction. J. Food Meas. Charact. 12 (4), 2718–2724. doi:10.1007/s11694-018-9889-y.

Wang, W., Bao, Y., Chen, Y., 2013. Characteristics and antioxidant activity of water-soluble Maillard reaction products from interactions in a whey protein isolate and sugars system. Food Chem. 139 (1), 355–361. doi:10.1016/j.foodchem.2013.01.072.

Wang, W.D., Li, C., Bin, Z., Huang, Q., You, L.J., Chen, C., Fu, X., Liu, R.H., 2020. Physicochemical properties and bioactivity of whey protein isolate-inulin conjugates obtained by Maillard reaction. Int. J. Biol. Macromol. 150, 326–335. doi:10.1016/j.ijbiomac.2020.02.086.

Wei, C.K., Ni, Z.J., Thakur, K., Liao, A.M., Huang, J.H., Wei, Z.J., 2019. Color and flavor of flaxseed protein hydrolysates Maillard reaction products: Effect of cysteine, initial pH, and thermal treatment. Int. J. Food Prop. 22 (1), 84–99. doi:10.1080/10942912.2019.1573830.

Weinbreck, F., de Vries, R., Schrooyen, P., de Kruif, C.G., 2003. Complex coacervation of whey proteins and gum arabic. Biomacromolecules 4 (2), 293–303. doi:10.1021/bm025667n.

Wen, C., Zhang, J., Qin, W., Gu, J., Zhang, H., Duan, Y., Ma, H., 2020. Structure and functional properties of soy protein isolate-lentinan conjugates obtained in Maillard reaction by slit divergent ultrasonic assisted wet heating and the stability of oil-in-water emulsions. Food Chem. 331, 127374. doi:10.1016/j.foodchem.2020.127374.

Xie, S., Liu, Y., Zeng, S., Niu, J., Tian, L., 2016. Partial replacement of fish-meal by soy protein concentrate and soybean meal based protein blend for juvenile Pacific white shrimp, Litopenaeus vannamei. Aquaculture 464, 296–302. doi:10.1016/j.aquaculture.2016.07.002.

Xu, Z.Z., Huang, G.Q., Xu, T.C., Liu, L.N., Xiao, J.X., 2019. Comparative study on the Maillard reaction of chitosan oligosaccharide and glucose with soybean protein isolate. Int. J. Biol. Macromol. 131, 601–607. doi:10.1016/j.ijbiomac.2019.03.101.

Ye, M.P., Zhou, R., Shi, Y.R., Chen, H.C., Du, Y., 2017. Effects of heating on the secondary structure of proteins in milk powders using mid-infrared spectroscopy. J. Dairy Sci. 100 (1), 89–95. doi:10.3168/jds.2016-11443.

Zha, F., Dong, S., Rao, J., Chen, B., 2019. The structural modification of pea protein concentrate with gum Arabic by controlled Maillard reaction enhances its functional properties and flavor attributes. Food Hydrocolloids 92, 30–40. doi:10.1016/j.foodhyd.2019.01.046.

Zha, F., Yang, Z., Rao, J., Chen, B., 2020. Conjugation of pea protein isolate via Maillard-driven chemistry with saccharide of diverse molecular mass: molecular interactions leading to aggregation or glycation. J. Agric. Food Chem. 68 (37), 10157–10166. doi:10.1021/acs.jafc.0c04281.

Zhang, B., Chi, Y.J., Li, B., 2014. Effect of ultrasound treatment on the wet heating Maillard reaction between β-conglycinin and maltodextrin and on the emulsifying properties of conjugates. Eur. Food Res. Technol. 238 (1), 129–138. doi:10.1007/s00217-013-2082-y.

Zhang, J.B., Wu, N.N., Yang, X.Q., He, X.T., Wang, L.J., 2012. Improvement of emulsifying properties of Maillard reaction products from β-conglycinin and dextran using controlled enzymatic hydrolysis. Food Hydrocolloids 28 (2), 301–312. doi:10.1016/j.foodhyd.2012.01.006.

Zhao, S., Huang, Y., McClements, D.J., Liu, X., Wang, P., Liu, F., 2022. Improving pea protein functionality by combining high-pressure homogenization with an ultrasound-assisted Maillard reaction. Food Hydrocolloids 126, 107441. doi:10.1016/j.foodhyd.2021.107441.

Zhou, X., Cui, H., Zhang, Q., Hayat, K., Yu, J., Hussain, S., Tahir, M.U., Zhang, X., Ho, C.T., 2021. Taste improvement of Maillard reaction intermediates derived from enzymatic hydrolysates of pea protein. Food Res. Int. 140, 109985. doi:10.1016/j.foodres.2020.109985.

Zhu, D., Damodaran, S., Lucey, J.A., 2008. Formation of whey protein isolate (WPI)-dextran conjugates in aqueous solutions. J. Agric. Food Chem. 56 (16), 7113–7118. doi:10.1021/jf800909w, Scopus.

Žilić, S., Akıllıoğlu, G., Serpen, A., Barać, M., Gökmen, V., 2012. Effects of isolation, enzymatic hydrolysis, heating, hydratation and Maillard reaction on the antioxidant capacity of cereal and legume proteins. Food Res. Int. 49 (1), 1–6. doi:10.1016/j.foodres.2012.06.031.